

Link between Perpendicular Coupling and Exchange Biasing in $\text{Fe}_3\text{O}_4/\text{CoO}$ Multilayers

Y. Ijiri,¹ T. C. Schulthess,² J. A. Borchers,³ P. J. van der Zaag,⁴ and R. W. Erwin³

¹*Department of Physics and Astronomy, Oberlin College, Oberlin, Ohio 44074, USA*

²*Center for Nanophase Materials Science and Computer Science and Mathematics Division, ORNL, Oak Ridge, Tennessee 37831-6114, USA*

³*NIST Center for Neutron Research, National Institute of Standards and Technology, Gaithersburg, Maryland 20899, USA*

⁴*Philips Research Laboratories, High Tech Campus 11, 5656 AA Eindhoven, The Netherlands*

(Received 22 January 2007; published 1 October 2007)

In studying well-characterized, exchange-biased $\text{Fe}_3\text{O}_4/\text{CoO}$ superlattices, we demonstrate a causal link between the exchange bias effect and the perpendicular coupling of the ferrimagnetic and antiferromagnetic spins. Neutron diffraction studies reveal that for thin CoO layers the onset temperature for exchange biasing T_B matches the onset of locked-in, preferential perpendicular coupling of the spins, rather than the antiferromagnetic ordering temperature T_N . The results are explained by considering the role of anisotropic exchange first proposed by Dzyaloshinsky and Moriya and developing a model based purely on information on structural defects and exchange for these oxides. The devised mechanism provides a general explanation of biasing in systems with perpendicular coupling.

DOI: [10.1103/PhysRevLett.99.147201](https://doi.org/10.1103/PhysRevLett.99.147201)

PACS numbers: 75.70.Kw, 75.50.Ee, 85.70.Kh

The exchange biasing phenomenon has been the focus of much attention [1,2]. First discovered 50 years ago [3], the effect refers to a field shift in a hysteresis loop as a result of exchange coupling between an antiferromagnetic (AF) and a ferro- or ferrimagnetic (F) material. Aspects of the microscopic origins of biasing remain unexplained, despite many theoretical investigations [4,5]. The most widely accepted models derive from Malozemoff's work [6], which noted that random interface roughness will naturally lead to interfacial exchange compensation, but that for finite size domains or grains, there will always be a net exchange interaction that leads to bias. This interaction will decrease with increasing domain size and vanish in the single domain limit.

To test these theories, exchange biasing has been studied in model systems with well-characterized interfacial spin structure. While some samples have displayed a parallel or antiparallel alignment of the F vs AF spins [7], for a few crystalline systems, the F spins align *perpendicular* to the AF spins [8,9] in the exchange-biased state. This can be shown to be a natural consequence of frustrated interfacial exchange [10,11], where the exchange field due to the F spins acts equally on all AF sublattices. However, for Heisenberg exchange, such a spin-flop coupling is *uniaxial* [12] and thus cannot contribute to the *unidirectional* bias effect. Furthermore, for interfaces with compensated F-AF exchange, Stiles and McMichael [13] have shown that for all but the smallest AF domains or grains, the F spins will align perpendicularly to the AF spins, a spin arrangement that is inconsistent with virtually all presently accepted mechanisms of exchange bias. In some systems, such as CoO/NiFe, this view is corroborated [14] as exchange bias appears to vanish in the limit of large grains and compensated interfaces. Experimental work on other systems has often revealed a noncollinear

alignment of F to AF spins [15,16], but the connection of these arrangements to exchange biasing has been difficult to establish.

In this Letter, we focus on addressing this issue by studying the biasing temperature dependence in ferrimagnetic magnetite $\text{Fe}_3\text{O}_4/\text{AF}$ cobalt monoxide CoO, a system for which we have previously shown [8] that exchange bias and perpendicular F-AF spin alignment *can* coexist. Because of the similarities in the oxygen sublattices of the spinel F and rock salt AF, high-quality epitaxial superlattices, amenable to neutron scattering, can be grown. We first report new experimental results, which unequivocally show that the perpendicular F-AF spin alignment and exchange bias are *directly* correlated, in that this AF spin alignment unfreezes around the blocking temperature T_B at which the bias field vanishes. Taking advantage of the clean epitaxy, we then present a microscopic spin-model based purely on structural and general exchange information for these oxides. The model highlights the role of anisotropic interfacial exchange [17,18] to provide a more general explanation of biasing in systems with perpendicular coupling.

The [001] epitaxial $\text{Fe}_3\text{O}_4(10\text{ nm})/\text{CoO}(1.7\text{--}10\text{ nm})$ multilayers for this study were grown on MgO substrates using molecular beam epitaxy, as described before [19]. Low angle x-ray and neutron reflectivity measurements confirmed the high quality of the interfaces, with interfacial full-widths at half maximum values of less than 1 nm. To determine T_B [20], hysteresis loops were measured after cooling the samples from 350 K in a 4400 kA/m field in a SQUID-based magnetometer. Neutron diffraction studies were performed at the NIST Center for Neutron Research using a triple axis spectrometer, with a 7 T superconducting magnet and a pyrolytic graphite monochromator and analyzer for neutrons of energy 14.8 meV.

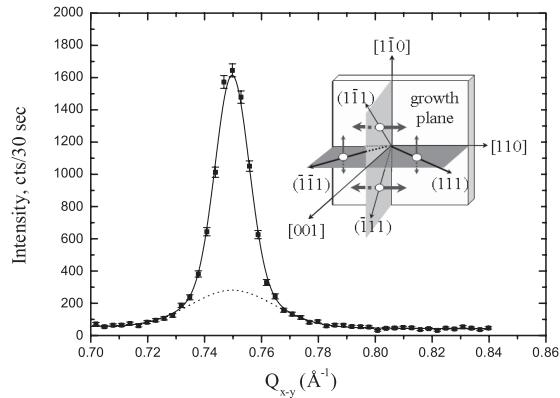


FIG. 1. Scan of the (111) reflection within the growth plane for a [10 nm $\text{Fe}_3\text{O}_4/3.0$ nm CoO] $_{50}$ multilayer film at 78 K. The reflection has a two-component line shape: the broad F component is denoted by a dotted line. Inset illustrates the AF spin structure consisting of the four labeled $\{111\}$ domains with spins alternating in the directions indicated by the double-tipped arrows.

The diffraction experiments focused on the field and temperature dependencies of the major AF (111) reflection. As illustrated in Fig. 1, this reflection has a broad component due to the Fe_3O_4 magnetic and structural order and a narrow component from the CoO AF order [8]. The broadened Fe_3O_4 width stems from antiphase boundaries (APBs) that are common in crystalline magnetite films [21,22] and can be easily separated from the narrow CoO component. These widths provide estimates for the F and AF domain sizes, respectively. Note also that APBs are present along the growth direction at each $\text{Fe}_3\text{O}_4/\text{CoO}$ interface [8,23]. From the FWHM of the two components, we have calculated that the magnetic AF domain sizes both across the sample plane (≥ 50 nm) and along the growth axis (≥ 50 –100 nm) are larger than the size of the Fe_3O_4 antiphase domains (≈ 30 nm and ≈ 10 nm respectively).

Our previous study [8] shows that the AF spins in these superlattices lie in ferromagnetic sheets which alternate sign along $\langle 111 \rangle$ propagation directions as in bulk CoO [24]. Unlike bulk, however, each $\{111\}$ domain has a unique easy axis, with spins lying within the (001) sample growth plane as shown in the inset to Fig. 1. Thus, in addition to indicating the presence of ordered AF spins as is usual for diffraction peaks, a comparison of the intensities of the $\{111\}$ reflections also indicates the average *direction* of these spins relative to an applied field.

As noted earlier, we have found that at low temperatures, the majority of the AF spins are frozen perpendicular to an applied magnetic field as a result of frustration due to interfacial exchange coupling to the F spins [8]. Now, we report results investigating the temperature dependence and by focusing on its onset, we try to understand its origin and relationship to exchange bias.

As illustrated in Fig. 2, we have tracked the CoO component of the (111) reflection intensity as a function of increasing temperature for two superlattices,

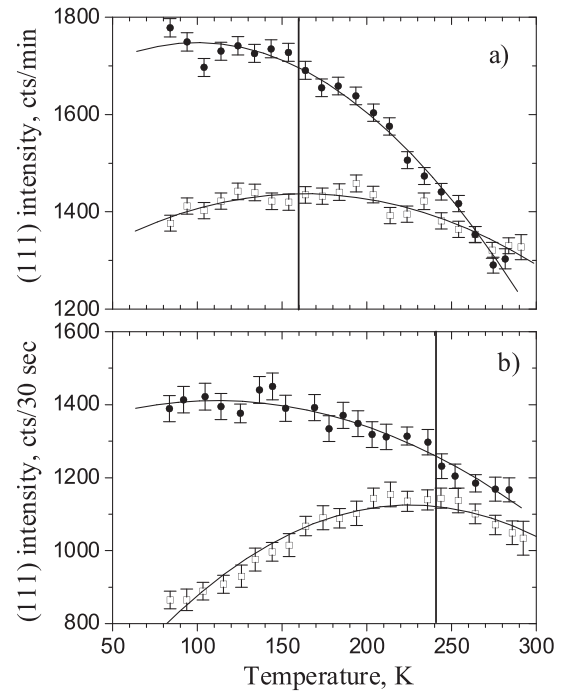


FIG. 2. Changes in the CoO component of the (111) reflection intensity as a function of increasing temperature for a) [10 nm $\text{Fe}_3\text{O}_4/1.7$ nm CoO] $_{50}$ and b) [10 nm $\text{Fe}_3\text{O}_4/3.0$ nm CoO] $_{50}$ multilayer films. The filled circles indicate data taken after cooling from room temperature in zero field, while the open squares indicate data taken in zero field after cooling the sample in 4000 kA/m field from room temperature to 78 K. The solid lines are guides to the eye; vertical lines indicate the blocking temperatures for the two samples as determined by magnetometry measurements.

[10 nm $\text{Fe}_3\text{O}_4/1.7$ nm CoO] $_{50}$ and [10 nm $\text{Fe}_3\text{O}_4/3.0$ nm CoO] $_{50}$, which have blocking temperatures significantly below their AF ordering temperatures (T_N values) of 510 ± 10 K and 450 ± 15 K, respectively, as determined by neutron diffraction measurements of AF peak intensity vs temperature. Specifically, the figure depicts the (111) intensity in zero field upon warming after cooling in zero field and in a 4000 kA/m field applied along the $[1\bar{1}0]$ direction. In the zero field case, all four $\{111\}$ AF domains [that give rise to the (111), $(\bar{1}\bar{1}1)$, $(1\bar{1}\bar{1})$, and $(\bar{1}\bar{1}\bar{1})$ reflections] are occupied equally. The zero field data on warming show the expected Brillouin-like falloff with increasing temperature as long-range order is reduced. In contrast, field cooling along the $[1\bar{1}0]$ direction leads to a preferential alignment of AF spins along the $[110]$ and as a result an *increase* in intensity in the $(1\bar{1}\bar{1})$ and $(\bar{1}\bar{1}\bar{1})$ reflections and a *decrease* in the (111) and $(\bar{1}\bar{1}1)$ reflections, considering the easy axes indicated in Fig. 1. The (111) reflection intensity, in particular, is weaker than the zero field case. Upon heating, the (111) reflection intensity for the field cooled case exhibits a broad maximum for both samples. At temperatures above the maximum, we have experimentally determined that the AF $\{111\}$ intensities are again equal for all four domains, indicating a randomizing of the

AF spins. Thus the broad feature arises from the competition between two effects: (1) the intensity decrease associated with the reduction of long-range order upon heating as noted for the zero field case and (2) the increase in intensity caused by the release of the frozen AF spins from their perpendicular orientation. This intensity increase stops when all the frozen AF spins are released, and thus, the temperature dependent intensities for the field cooled experiment must go through a maximum at or below this temperature. As is clear from Fig. 2, this maximum occurs at different temperatures in the two samples and correlates with the blocking temperatures measured independently by SQUID magnetometry methods.

The behavior for the samples with $T_B < T_N$ contrasts with that observed for a $[10 \text{ nm Fe}_3\text{O}_4/10 \text{ nm CoO}]_{50}$ superlattice in which T_B ($290 \pm 10 \text{ K}$ extracted from hysteresis loops) approximates T_N ($325 \pm 15 \text{ K}$ measured with neutron diffraction). When a large magnetic field is applied in the $[1\bar{1}0]$ direction after cooling in zero field, we find again that the (111) intensity decreases as the AF spins align perpendicular to the field and the F moment direction. However, in this case, upon warming in zero field, no thermally induced reorientation of the AF spins is observed as $T_B \sim T_N$. Instead, the AF spins show memory of the field preparation due to the magnetized Fe_3O_4 spins. Randomizing the F spins by ac cycling of the field is necessary to restore an equal population to the $\{111\}$ AF domains. Note that these data indicate that the F-AF coupling primarily establishes the CoO spin structure as opposed to the applied magnetic field.

Taken together, the results presented here link the onset of exchange biasing at T_B with the freezing of perpendicular F-AF spin alignment, thus requiring a common microscopic origin for the two effects in $\text{Fe}_3\text{O}_4/\text{CoO}$. We will now show that a straightforward microscopic explanation [17] can be given with a model built solely from structural and magnetic exchange considerations, along with our measurements of characteristic domain sizes.

The interfacial structure is relatively simple due to the matching O sublattices. Figure 3 depicts two of four possible configurations that arise from different Fe_3O_4 antiphase domains. The tetrahedral Fe atoms lie between the O atoms (on A sites), while the octahedral Fe atoms occupy equivalent sites as the Co (both B sites). Given this structure, it is reasonable to assume that there are superexchange interactions: (1) J_{AB} , between nearest neighbor tetrahedral Fe and octahedral Co and (2) J_{BB} , between nearest neighbor octahedral Fe and Co, with J_{AB} the dominant one, as for similar oxides [25]. The interfacial exchange energy per Fe-Co pair can be written as

$$\mathcal{E}_{\text{exch}}^{i=\text{Co},j=\text{Fe}} = -J_{AB}[\vec{s}_i \cdot \vec{s}_j + \vec{D}_{AB}^{ij}/J_{AB} \cdot (\vec{s}_i \times \vec{s}_j)].$$

Note, in particular, that the Dzyaloshinsky-Moriya (DM) term, \vec{D}_{AB}^{ij} , which usually vanishes in bulk crystals due to symmetry [26], has to be included because of symmetry breaking at the interface of these films [18].

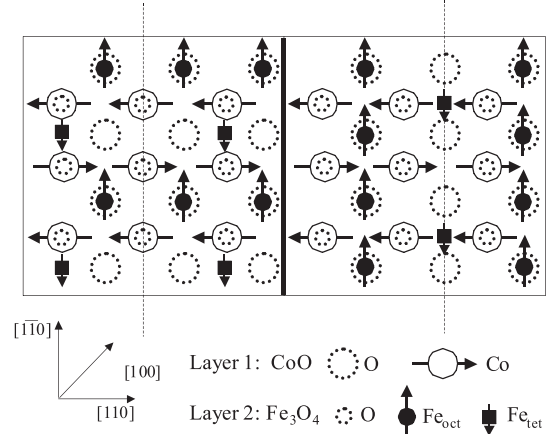


FIG. 3. Two possible atomic configurations of the $\text{Fe}_3\text{O}_4/\text{CoO}$ interface, separated by an APB. The dashed lines represent mirror symmetry planes for each individual antiphase domain.

Given that the observed CoO structural domain size is much larger than the magnetic one at all temperatures, we will restrict the discussion to single crystals. Within each (001) Fe_3O_4 plane, the rows of octahedral Fe atoms are aligned either along the $[1\bar{1}0]$ and the $[110]$ directions, as are the CoO easy axes. Multiple antiphase domains in the Fe_3O_4 layer will result in interface structures typified [21,22] by the APB shown in Fig. 3. Since the CoO AF domain sizes are larger than those for the Fe_3O_4 antiphase domains (e.g., Fig. 1), we model a single CoO AF domain extending over the sides of the APBs and coupling to tetrahedral Fe in different sublattices (e.g., across the boundary in Fig. 3). As a result, the net exchange per AF domain is compensated and the total interfacial exchange energy is minimized when the Co moments align perpendicular to the Fe_3O_4 , due to the DM term. Consistent with our data and Fig. 3, $(1\bar{1}1)$ and $(\bar{1}11)$ type domains are preferred for large fields along $[1\bar{1}0]$.

If there were no APBs, the interfacial Co and adjacent tetrahedral Fe sites would be in a mirror plane perpendicular to the interface. Consequently [26], \vec{D}_{AB}^{ij} would be perpendicular to this mirror plane and its component perpendicular to the interface would vanish, i.e. $\vec{D}_{AB,\perp}^{ij} = 0$. In our sample, however, at least 10% of the tetrahedral Fe sites are at APBs, where the mirror symmetry is broken and $\vec{D}_{AB,\perp}^{ij} \neq 0$. When the Fe and Co moments are perpendicularly aligned and parallel to the interface, every tetrahedral Fe-Co pair contributes $\Delta\mathcal{E}_{\text{exch}}^{ij} \approx 2D_{AB,\perp}^{ij}$ to the energy difference between the two respective states when the Fe moments are reversed. The total energy difference depends on the relative size and sign of different $\vec{D}_{AB,\perp}^{ij}$ pairs, which in turn requires more detailed knowledge of the interface. To estimate if this symmetry breaking can account for exchange bias, we consider two cases and compare the net unidirectional coupling to the random field Ising model [6]: (1) When the antiphase domains are very intertwined with random shape as shown in Ref. [22], we can assume

that $\vec{D}_{AB,\perp}^{ij}$ is a random vector with random length. For this case we have shown with numerical simulations [17], that symmetry breaking due to the DM interaction is somewhat smaller but still comparable to that in the random field Ising model [6], which is generally accepted to give the correct exchange bias magnitude [13]. In fact, for sufficiently large enough AF domains, as in this case, the simulations show that all AF moments are nearly along the AF easy axis and all F moments are nearly along the perpendicular coupling direction. For this case, the energy difference per tetrahedral Fe-Co pair upon F moment reversal is well approximated by $\Delta E^{(1)} \approx \sqrt{\frac{2}{N}}D$, where N is the number of tetrahedral Fe-Co pairs. The corresponding result for the random field Ising model is $\Delta E_{\text{Ising}} \approx \frac{2}{\sqrt{N}}J_{AB}$, leaving us with $\Delta E^{(1)}/\Delta E_{\text{Ising}} \approx \sqrt{1/2} \frac{D}{J_{AB}}$. Moriya [26] estimated $D/J \approx 0.1$ in bulk AFs, but larger values (≈ 0.5) have been reported in systems with lower symmetry [27]. Therefore, the net coupling field per AF domain due to a random DM interaction is only about 3 to 4 times smaller than for the random field Ising model. (2) When the antiphase domains have smooth boundaries, $\vec{D}_{AB,\perp}^{ij}$ will be very small for Fe atoms away from the APB since the mirror symmetry is locally restored. At the APBs, there will be segments where the local environments of the tetrahedral Fe atoms are similar, hence leading to similar $\vec{D}_{AB,\perp}^{ij}$. The segments thus act as extended defects where the DM interaction yields a net unidirectional coupling in the direction perpendicular to the AF spins, denoted by $\vec{D}_s = \sum \vec{D}_{AB,\perp}^{ij}$ for the segment. Since the AF domains cover several antiphase domains, \vec{D}_s can again be viewed as a random variable. The energy difference per tetrahedral Fe-Co pair upon reversal of the F moments is then given by $\Delta E^{(2)} \approx \sqrt{\frac{2}{n_s}}Dx$, where n_s is the average number of segments and x the fraction of tetrahedral atoms at the APBs. In our case with $x \sim 0.1$ and $n_s \sim 8$, we find $\Delta E^{(2)}/\Delta E^{(1)} = \sqrt{\frac{N}{n_s}} * 0.1 \approx 3$.

Note that in either case, the coupling derived from DM exchange is of similar magnitude as in the random field Ising model. Therefore, we have identified a possible mechanism for unidirectional coupling that coincides with the perpendicular coupling and hence explains the strict correlation between the two observed in the neutron scattering experiments.

In summary, our neutron diffraction measurements indicate that the Co spins in $\text{Fe}_3\text{O}_4/\text{CoO}$ superlattices are preferentially frozen perpendicular to the Fe spins only at and below T_B for thin CoO layers. The reduced blocking temperatures for these samples are correlated with the onset of biasing behavior and not with a reduction of T_N [20]. Within the context of anisotropic exchange originating from the symmetry-breaking APBs in the F layers, we have demonstrated that the freezing of the perpendicular coupling appears to be responsible for exchange biasing in

this system, as our results are of similar magnitude to the random field Ising model. The present work highlights the need for complete analysis of the interfacial atomic and magnetic structure in order to determine the biasing mechanism in F/AF systems.

We thank R. M. Wolf for the sample preparation and L.F. Feiner for many useful discussions. This research was partially supported by the donors of the Petroleum Research Fund, administered by the ACS and by the division for Scientific User Facilities of the U. S. Department of Energy.

-
- [1] J. Nogués and Ivan K. Schuller, *J. Magn. Magn. Mater.* **192**, 203 (1999).
 - [2] A. E. Berkowitz and K. Takano, *J. Magn. Magn. Mater.* **200**, 552 (1999).
 - [3] W. H. Meiklejohn and C. P. Bean, *Phys. Rev.* **102**, 1413 (1956); **105**, 904 (1957).
 - [4] M. Kiwi, *J. Magn. Magn. Mater.* **234**, 584 (2001).
 - [5] R. L. Stamps, *J. Phys. D* **33**, R247 (2000).
 - [6] A. P. Malozemoff, *Phys. Rev. B* **37**, 7673 (1988).
 - [7] H. Ohldag, H. Shi, E. Arenholz, J. Stöhr, and D. Lederman, *Phys. Rev. Lett.* **96**, 027203 (2006).
 - [8] Y. Ijiri *et al.*, *Phys. Rev. Lett.* **80**, 608 (1998); *J. Appl. Phys.* **83**, 6882 (1998).
 - [9] T. J. Moran, J. Nogués, D. Lederman, and Ivan K. Schuller, *Appl. Phys. Lett.* **72**, 617 (1998).
 - [10] L. L. Hinchey and D. L. Mills, *Phys. Rev. B* **34**, 1689 (1986).
 - [11] N. C. Koon, *Phys. Rev. Lett.* **78**, 4865 (1997).
 - [12] T. C. Schulthess and W. H. Butler, *Phys. Rev. Lett.* **81**, 4516 (1998).
 - [13] M. D. Stiles and R. D. McMichael, *Phys. Rev. B* **59**, 3722 (1999).
 - [14] N. Gökemeijer, R. L. Penn, D. R. Veblen, and C. L. Chien, *Phys. Rev. B* **63**, 174422 (2001).
 - [15] F. Stromberg, W. Keune, V. E. Kuncser, and K. Westerholt, *Phys. Rev. B* **72**, 064440 (2005).
 - [16] H. Matsuda, S. Okamura, T. Shiosaki, H. Adachi, and H. Sakakima *et al.*, *J. Appl. Phys.* **98**, 063903 (2005).
 - [17] T. C. Schulthess, *Mater. Res. Soc. Symp. Proc.* **346**, 31 (2003).
 - [18] A. Crépieux and C. Lacroix, *J. Magn. Magn. Mater.* **182**, 341 (1998).
 - [19] R. M. Wolf *et al.*, *Mater. Res. Soc. Symp. Proc.* **341**, 23 (1994).
 - [20] P. J. van der Zaag *et al.*, *Phys. Rev. Lett.* **84**, 6102 (2000).
 - [21] D. T. Margulies, F. T. Parker, M. L. Rudee, F. E. Spada, J. N. Chapman, P. R. Aitchison, and A. E. Berkowitz, *Phys. Rev. Lett.* **79**, 5162 (1997).
 - [22] T. Hibma *et al.*, *J. Appl. Phys.* **85**, 5291 (1999).
 - [23] J. A. Borchers *et al.*, *Phys. Rev. B* **51**, 8276 (1995).
 - [24] W. L. Roth, *Phys. Rev.* **110**, 1333 (1958).
 - [25] A. Broese van Groenou, P. F. Bongers, and A. L. Stuyts, *Mater. Sci. Eng.* **3**, 317 (1969).
 - [26] I. Dzyaloshinsky, *Sov. Phys. JETP* **5**, 1259 (1957); T. Moriya, *Phys. Rev.* **120**, 91 (1960).
 - [27] M. I. Katsnelson, V. V. Dobrovitski, and B. N. Harmon *et al.*, *J. Appl. Phys.* **85**, 4533 (1999).